



Orientation Distribution of Molecules: Characterization and Experimental Determination by Means of Magnetic Resonance

Natalia A. Chumakova¹ · Andrey Kh. Vorobiev¹

Received: 25 June 2020 / Revised: 2 August 2020 / Published online: 12 October 2020
© Springer-Verlag GmbH Austria, part of Springer Nature 2020

Abstract

The article presents a comparative review of experimental methods used for characterization of orientational ordering of the molecules in a partially aligned media. The optical, X-ray and magnetic resonance techniques are considered. The potential and limitations of different approaches are discussed. The magnetic resonance is concluded to be the most informative technique for detailed characterization of the molecular orientation distribution.

1 Introduction

Interest on determination of the orientational molecular alignment is growing now in course of the extensive fundamental study of spatially organized media and the design of new applied materials. The properties of substances and materials organized at molecular level such as stretched polymers, liquid crystals, biological or synthetic membranes etc. are largely governed by the orientational ordering of molecules. In this regard, urgent problem for physical chemistry and chemical physics is the development of experimental methods for the quantitative structural characterization of the partially ordered soft matter. This review is devoted to the comparative description of various methods for study of the partially ordered materials.

At present, the most common methods used for the experimental characterization of the molecular orientational ordering are birefringence, various types of optical spectroscopy, X-ray absorption and diffraction, as well as nuclear magnetic resonance (NMR) and electron paramagnetic resonance (EPR). In the present review the comparative analysis of various approaches developed for characterization of the orientational ordering is presented. We will show that magnetic resonance spectroscopy is the most

✉ Natalia A. Chumakova
harmonic2011@yandex.ru

¹ Chemistry Department, Moscow State University, Leninskie Gory 1-3, Moscow 119991, Russia

informative method for investigation of systems with sophisticated orientation distribution of molecules.

2 Quantitative Description of Molecular Orientational Ordering

There are various ways to describe of the orientational ordering of molecules in a sample. The most frequently used characteristics of the molecular orientational alignment are the orientation distribution function, the Herman's orientation factors, the elements of Saupe matrix and the White–Spruiell orientation factors. The detailed description of these functions is presented in [1–4].

The orientation of a molecule with the arbitrary symmetry relative to the sample coordinate system can be specified by the three Euler angles (α, β, γ) that transform the sample reference frame to the molecule reference frame. The most detailed characteristic of the orientational ordering is the orientation distribution function $\rho(\alpha, \beta, \gamma)$. The orientation distribution function (ODF) can be represented as a series of the generalized spherical harmonics:

$$\rho(\alpha, \beta, \gamma) = \sum_{j,m,l} \frac{2j+1}{8\pi^2} P_{jml} D_{ml}^j(\alpha, \beta, \gamma), \quad (1)$$

where D_{ml}^j are the generalized spherical functions (Wigner functions); P_{jml} are the expansion coefficients termed orientation moments or orientation order parameters of the j th rank.

The spatial orientation of an axial molecule is uniquely defined by two angles specifying the orientation of the molecular axis in the sample coordinate frame. In this case, the orientation distribution function can be expressed by a series of spherical harmonics:

$$\rho(\beta, \gamma) = \frac{1}{2\pi} \sum_{j=0}^{\infty} \left[\frac{1}{2} a_{j0} P_j(\cos \beta) + \sum_{m=1}^j P_{jm}(\cos \beta) (a_{jm} \cos(m\gamma) + b_{jm} \sin(m\gamma)) \right], \quad (2)$$

where $P_j(\cos \beta)$ are the Legendre polynomials; $P_{jm}(\cos \beta)$ are the associated Legendre functions; a_{jm} , b_{jm} are real coefficients.

The distribution function of the molecules with arbitrary symmetry in an axial sample is described by the same expression (2). In this case, the angles (β, γ) define the orientation of sample axis in the molecular frame. In the case of the orthorhombic molecular symmetry, in the series (2) only the a_{jm} with even indices j and m are nonzero.

The orientation distribution of axial molecules in axial sample is described by a series of Legendre functions:

$$\rho(\beta) = \sum_{j=0}^{\infty} \left[\frac{1}{2} a_{j0} P_j(\cos \beta) \right]. \quad (3)$$

Other method of description of the molecular orientation distribution is based on the Herman's orientation factors. These values specify the average orientation of any molecular axis relative to chosen axis of sample. So, the Herman's orientation factor of the molecular X'' axis relative to the sample Z' axis is given by the following expression:

$$f_{X''/Z'} = \frac{3\langle \cos^2 \beta \rangle - 1}{2}, \quad (4)$$

where β is the angle between the molecular axis X'' and the sample Z' axis; angular brackets denote averaging over all molecules.

The complete set of the Herman's factors consists of nine quantities. They are not independent, since the sum of squared cosines of the angles between any molecular axis and three sample coordinate axes is equal to unity. There are only four independent Herman's factors related to the four independent second-rank coefficients P_{200} , P_{220} , P_{202} and P_{222} in the series (Eq. 1) [4].

The orientational ordering of molecules in an axial sample is often characterized using elements of the Saupe matrix, defined as follows:

$$S_{ij} = \frac{\langle 3 \cos \theta_{in} \cos \theta_{jn} - \delta_{ij} \rangle}{2}, \quad (5)$$

where θ_{in} and θ_{jn} are the angles between the molecular axes i and j correspondently and the sample axis.

Obviously, there are five independent elements of the Saupe matrix. The relation of these elements to the orientation order parameters is presented in [3]. For molecules with the point symmetry groups C_{2v} , D_2 , and D_{2h} there are two independent elements of the Saupe matrix $S = S_{zz}$ and $G = S_{xx} - S_{yy}$.

The White–Spruiell orientation factors are used to characterize the predominant ordering along two different sample axes. These parameters show the average orientation of one of the molecular axes with respect to the two sample axes. For example, the values

$$f_{X''/X'}^B = 2\langle \cos^2 \theta_{X''/X'} \rangle + \langle \cos^2 \theta_{X''/Z'} \rangle - 1 \quad (6a)$$

$$f_{X''/Z'}^B = 2\langle \cos^2 \theta_{X''/Z'} \rangle + \langle \cos^2 \theta_{X''/X'} \rangle - 1 \quad (6b)$$

characterize the average orientation of the X'' molecular axes relative to the X' and Z' sample axes. The White–Spruiell orientation factors are explicitly related to the Herman's orientation factors [4].

Different characteristics of the orientational ordering are appropriate for treatment of different experimental data or for description of different type of order. However, the order parameters defined by the orientation distribution function (1) are most suitable for comparing results of different methods.

3 Optical methods of Characterization of The Orientational Molecular Ordering

Optical methods are based on the interaction of electromagnetic radiation with substance. An important value describing this interaction is the complex refractive index $\hat{n} = n - ik$, where n is the real refractive index dictated by molecular polarizability and k is the absorption coefficient.

Both the polarizability and the absorption coefficient are anisotropic characteristics dependent on the direction of the electric vector of electromagnetic wave in the molecular coordinate system. For this reason, the optical characteristics of the sample formed by orientationally ordered molecules depend on the orientation of the sample relative to direction and polarization of electromagnetic wave. By measuring the anisotropy of the optical constants one can determine the degree of molecular ordering in the sample.

3.1 Birefringence

The birefringence is the difference in the refractive indices of electromagnetic radiation with different polarizations. The differences between the refractive indices measured for three mutually perpendicular directions of electric vector of light (X' , Y' , Z') are related to the second-rank moments of the orientation distribution function by the following eq. [4]:

$$\Delta n_{Z'/X'} = n_{Z'} - n_{X'} = \Delta^0(P_{200} + 2P_{220}) + \delta^0(3P_{202} + P_{222}) \quad (7a)$$

$$\Delta n_{Z'/Y'} = n_{Z'} - n_{Y'} = \Delta^0(P_{200} - 2P_{220}) + \delta^0(3P_{202} - P_{222}) \quad (7b)$$

$$\Delta n_{X'/Y'} = n_{X'} - n_{Y'} = 4\Delta^0 P_{220} + 2\delta^0 P_{222}, \quad (7c)$$

where $\Delta^0 = n_{Z'}^0 - \frac{1}{2}(n_{X'}^0 + n_{Y'}^0)$; $\delta^0 = n_{X'}^0 - n_{Y'}^0$; $n_{X'}^0, n_{Y'}^0, n_{Z'}^0$ correspond to perfect molecular alignment.

Equations 7a–c contain four independent values of P_{2ml} . Therefore, to determine the orientational moments (order parameters), it is necessary to carry out additional measurements by means other methods. If the axial molecules are studied, the values of δ^0 , P_{202} , and P_{222} are equal to zero and the birefringence data define two second-rank moments of the orientation distribution function. In the simplest case of the axial sample formed by axial molecules, the orientational ordering is characterized by a single value $P_{200} = \frac{n_{//} - n_{\perp}}{\Delta^0}$, where $n_{//}$ and n_{\perp} are the refractive indices in the directions parallel and perpendicular to the sample symmetry axis, Δ^0 is the difference between refraction indexes for perfectly oriented sample. For example, the birefringence method was used for study of the dependence of the order parameter P_{200} on the degree of axial tension of polyethylene [5]. The authors of [6] investigated the SmA–N phase transition of 8CB liquid crystal with use of birefringence. It should be noted that Δ^0 cannot be determined by direct measurement. Most often,

this value is estimated by extrapolating of the temperature dependence of refraction to absolute zero [7]. There are examples of determination of Δ^0 by parallel measurements of the birefringence and the speed of sound [8]. It is clear that the value of Δ^0 is always determined with significant uncertainty. For this reason, the birefringence measurements are often used only for qualitative considerations of the orientational ordering without quantitative determination of the order parameters [9–13].

The significant advantage of the birefringence measurements is high time resolution reaching nanosecond time range [14]. The birefringence is a “global” method that does not distinguish the ordering of different parts of sample. This disadvantage can be overcome to some extent by division of sample into fragments and studying the fragments individually. For instance, authors [15] used birefringence for investigation of the orientation of polymer chains in the films with different thickness. The localization of the ordered layer was determined as a result (Fig. 1). This example also demonstrates the high sensitivity of the birefringence method, that is suitable for examination of low ordered media.

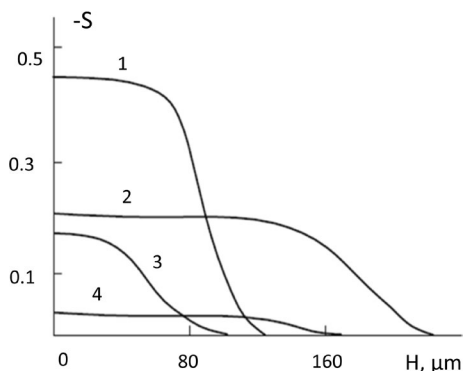
The division of the sample into separate fragments can also be used in the cases of other “global” methods. We will further not return to discussion of this issue. However, it should be noted that this approach cannot guarantee preservation of fragment ordering in the course of division procedure.

3.2 IR, UV–Visible Spectroscopy and Polarization Fluorescence

The determination of the molecular orientational ordering by absorption or emission of the light in ultraviolet, visible, or infrared range are based on the anisotropy of transition dipole moments. Probability of an optical transition is well known to be dependent on the angle between transition moment and the electrical component of radiation. Hence, the absorption/emission intensity is dictated by the orientation distribution of the transition moments and by the direction of electrical component of radiation.

The measurements of intensity for single-photon processes provide possibility to determine only the second-rank order parameters. Calculation of the P_{2ml} values is carried out in accordance with the Legendre addition theorem [16]:

Fig. 1 Order parameter P_{20} (S) over the thickness of the films: 1–polyimide, 2–cyclolinear polyphenyl sesquioxane, 3–polyamidoimide, 4–polystyrene. Reproduced from [15] with permission of “Phisics-Uspekhi” journal



$$P_{200}^{\text{sam}} = P_{200}^{\text{mol}}P_{200} + 12P_{220}^{\text{mol}}P_{202} \quad (8a)$$

$$P_{220}^{\text{sam}} = P_{200}^{\text{mol}}P_{220} + 2P_{220}^{\text{mol}}P_{222}, \quad (8b)$$

where P_{2ml}^{sam} are the order parameters of transition moments in the sample frame; P_{2ml}^{mol} are the order parameters of transition moments in the molecular frame; P_{2ml} are the order parameters of molecules in the sample frame.

Equations 1, 8a show that the determination of all second-rank order parameters is possible when using two different vibrational or electronic transitions jointly.

A typical IR spectrum is the dependence of the transmittance $T=I/I_0$ or the absorption $A=-\log T$ of the sample on radiation wavelength. As an illustration, Fig. 2a shows the difference in intensity of IR absorption of polyacrylonitrile fibers for different orientations of the radiation electric vector relative to the fiber axis [17]. The temperature dependence of the order parameter P_{200} designated as f is presented in Fig. 2b.

The works [18, 19] are the examples of use of near-IR and far-IR ranges, respectively, for characterization of the orientational properties of polymer materials. Since IR spectroscopy is sensitive to the phase state, it is possible to characterize the orientational order of crystalline and amorphous phases of the polymer material independently [20, 21].

As a rule, the absorption coefficients of infrared radiation are high. Therefore, experiments in transmission mode are limited by thickness of sample. On the other hand, this feature permits to record spectra of thin layers and to determine the change of molecular order along the depth of sample [22]. The attenuated total reflection spectra are used for determination of ordering for the molecules adsorbed on a surface [23] as well as for measurement of the change of orientation distribution within first few micrometers of the sample [4, 21, 24]. An advantage of the front-surface specular reflection infrared spectroscopy is the ability to measure the orientational dependence of the strongest IR lines [25, 26]. The infrared

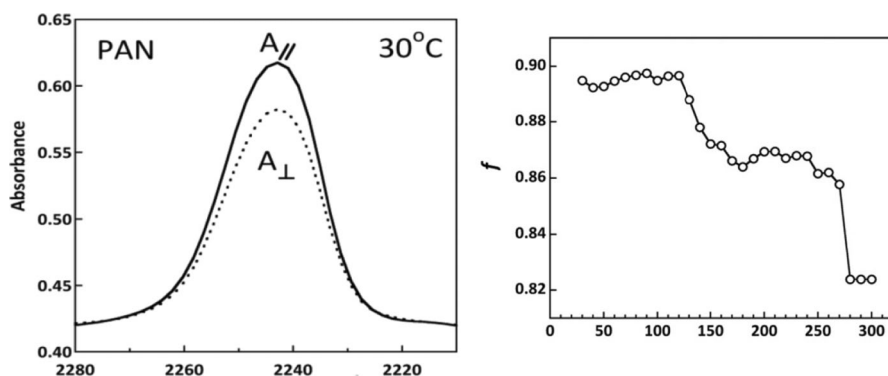


Fig. 2 Polarized IR spectra of the $\nu_{C\equiv N}$ bond of polyacrylonitrile (left), the temperature dependence of order parameter (right). Reproduced from [17] with permission of SAGE Publishing

reflection–absorption spectroscopy (IRRAS) is widely used in the case of thin films [27–29]. The method is based on measurement of the radiation passed through layer of substance but reflected by the layer–substrate interface. If degree of orientational alignment is low, the difference of absorption of radiation with different polarizations is small and can hardly be recorded. In such cases the modulation of polarization of IR radiation (PM–IRRAS) is used. This method is described in detail in [30, 31]. It can significantly increase the sensitivity of IR spectroscopy in the cases of polymers with small degrees of deformation, ultrathin films, etc. The Fourier transform IR spectroscopy is appropriate for monitoring the processes with time resolution from several milliseconds [32] to tens of microseconds [33].

UV–Vis spectroscopy differs from the IR spectroscopy significantly, because UV band, as a rule, is a superposition of several vibronic transitions. For this reason, the absorption of UV–Vis light is characterized by a tensor. The difference of UV–Vis absorption for different directions of light polarization is ordinarily called linear dichroism. The values characterizing the average orientation of the molecular axes relative to the sample axes in the case of UV–Vis spectroscopy are defined by different authors in different ways, but they are traditionally called order parameters. Thus, in [34] orientation distribution of axial molecules in a sample of arbitrary symmetry is described by values $S_{XY} = (\langle 3 \cos \theta_{Xa} \cdot \cos \theta_{Ya} - \delta_{XY} \rangle) / 2$, where θ_{Xa} and θ_{Ya} are the angles between the X or Y axes of the sample and the molecular anisotropy axis, δ_{XY} is Kronecker symbol; angle brackets mean averaging over all molecules. Obviously, the diagonal elements of the S_{XY} tensor are Herman's orientation factors. The authors of the classical work [35] define the orientation distribution of molecules with arbitrary symmetry in axial sample using the parameters $K_X = \langle \cos^2 \theta_{XA} \rangle$, $K_Y = \langle \cos^2 \theta_{YA} \rangle$, $K_Z = \langle \cos^2 \theta_{ZA} \rangle$, where θ_{XA} , θ_{YA} , θ_{ZA} are the angles between the X , Y , Z axes of the molecules and the sample anisotropy axis. In the general case of arbitrary symmetry sample formed by arbitrary symmetry molecules, each element of orientation tensor has four indices and describes the average orientation of two molecular axes relative to two sample axes [36, 37].

To study the orientational ordering, the dye characterized by high absorption coefficient and significant anisotropy of absorption tensor is often added to studied medium. It is important to keep in mind that correspondence between the dopant ordering and the molecular ordering of medium depends on many factors: geometry of the dye and medium molecules, their interaction, etc. Moreover, the dopant molecules can influence the orientational ordering of medium. Despite these drawbacks, use of dyes for measurement of the orientational ordering is the widespread approach. For example, dyes of various structure are often used to measure the order parameter of liquid crystals [38–40]. Polarized UV–Vis spectroscopy is widely used for investigations of biological objects [41–45]. A relatively new approach is the measurement of linear dichroism in a Couette flow (flow linear dichroism). In such a way the mutual orientation of protein fragments [46], the structure of DNA complexes with carbon nanotubes [47], and the structure of bacteriophages [48] were investigated.

Unlike IR and UV–Vis spectroscopy, fluorescence is characterized by two transition moments: the absorption transition moment and the emission transition moment. Thus, the polarized fluorescence alone provides information for determination of the

order parameters of the second and fourth ranks [49–52]. Since most substances are not capable of fluorescence, a small (about 100 ppm by mass [4, 53]) amount of fluorescent dye is introduced into orientationally ordered matrix. In rare cases, the matrix molecule itself contains a fluorescent group [4]. The fluorescent probes in polymer materials are mainly accumulated into the non-crystalline region of polymer, thus the obtained data correspond to the orientation of the molecules in the amorphous phase [54, 55]. If the lifetime of the excited state of dye exceeds the rotational correlation time, investigations of the rotation mobility is possible by measurement of relaxation of the orientational ordering [56, 57]. Of particular interest are the determination of sixth rank order parameters by polarized fluorescence. To obtain the values of P_{20} , P_{40} , and P_{60} , it is necessary to simultaneously determine the orientation of three different transition moments of molecule. It has been performed by the two-photon absorption of light which causes fluorescence of the dye molecule [58, 59]. The combination of spectrometer with a confocal microscope allows recording of spectrum within distinct thin layers of the sample. This method is used in the cases of fluorescence [60] and Raman spectroscopy [61, 62].

3.3 Raman Spectroscopy

Raman spectroscopy allows observing the vibrational transitions in non-polar groups of atoms (C–C, C=C, etc.). The main molecular characteristic in Raman spectroscopy is the polarizability tensor connecting the vector of electric field and the dipole moment induced by this field. To determine the orientational ordering of molecules, it is necessary to analyze the set of spectra recorded for various combinations of the relative direction and polarization of exciting and scattered light. Thus, both experimental technique and experimental data processing in the case of Raman spectroscopy are much more complicated than in the case of IR spectroscopy. The potential of Raman spectroscopy in measurement of the orientation distribution consists in the determination of the fourth rank order parameters in addition to the second-rank parameters [63–67]. It was shown [68] that the values of order parameters determined by analysis of various vibrational modes of molecule can be somewhat different.

Of great interest are measurements of the orientational ordering by simultaneous using of several methods. For example, orientational ordering of the fluorescent dye 4-dimethylamino-4'-nitrostilbene (DANS) in homological series of liquid crystals nCB ($n=5-9$), nOCB ($n=4-9$), nPCH ($n=3-10$), nCHBT ($n=3-9$) were studied using optical dichroism, polarized fluorescence, and Raman spectroscopy [69]. Figure 3 shows the temperature dependences of order parameters obtained by various methods. On can see that difference in the values of P_{20} and P_{40} obtained by different methods is comparable with the experimental uncertainty.

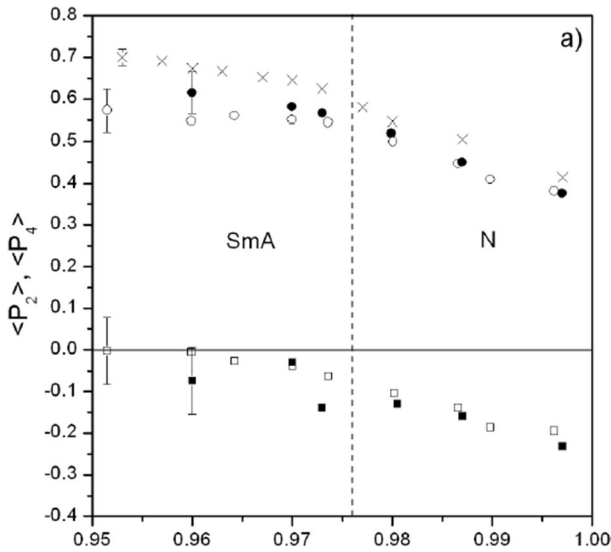


Fig. 3 Dependence of order parameters P_{20} and P_{40} on reduced temperature $T_{red} = T/T_{NI}$ for liquid crystals 8CB doped by DANS determined from absorption (crosses— P_{20} only), fluorescence measurement (black circles— P_{20} , black squares— P_{40}) and for respective liquid crystals obtained from Raman scattering measurements (white circles— P_{20} , white squares— P_{40}). Reproduced from [69] with permission of Polish Academy of Sciences, Institute of Physics

4 Absorption and Diffraction of X-rays

4.1 NEXAFS

Probability of electron transition upon absorption of X-rays, like absorption of IR and UV radiation, is defined by squared cosine of the angle between the transition moment and the electrical component of radiation. Therefore, the dependence of absorption intensity on polarization contains information about the molecular orientational ordering. The angular dependence of NEXAFS (Near Edge X-Ray Absorption Fine Structure) spectra is also called X-ray dichroism. Like IR and UV spectroscopy, NEXAFS is appropriate for determination of the second-rank order parameters only.

As free electrons are generated from depth of no more than 2 nm, NEXAFS is the surface-sensitive technique. This method is mainly used to study the orientational ordering of thin polymer films [70–74], carbon materials [75, 76] and liquid crystals [77, 78]. The surface sensitivity of NEXAFS is successfully used for detection of difference in ordering of different layers of material [76, 77]. It should be noted that NEXAFS is most often used for the qualitative characterization of material without quantitative estimation of order parameters. In the case of small ordering the interpretation of the NEXAFS experimental results is proved to be complicated and imprecise [74].

NEXAFS provides information on orientational ordering of various functional groups. The reliability of obtained data is largely determined by the correctness of

spectrum bands assignment. At present, the assignment became more reliable due to rapid development of quantum chemistry. The quantum chemistry methods allow theoretical calculation of the angular dependence of the NEXAFS spectra. As an illustration, Fig. 4 shows the experimental and predicted angular dependences of NEXAFS spectra for the orientationally ordered polymer [71].

4.2 X-Ray Diffraction

X-ray diffraction (XRD) is the best known method for study of crystalline substances. At present, XRD is also used to study partially ordered media, most often polymer materials and liquid crystals. The wide diffuse halos are observed in X-ray diffraction patterns of the amorphous materials instead of intense crystalline reflections. The order parameters of high ranks theoretically can be determined by analysis of the X-ray diffraction images [4]. In practice, only the second and, more rarely, the fourth rank order parameters are determined [4, 79–83]. As an illustration, Fig. 5 demonstrates the diffraction pattern of the nylon 6 fiber and the result of its simulation [84].

It should be noted that methods of treatment of diffraction patterns in the cases of partially ordered systems are continuously developing. New analysis technique mainly based on baseline correction was proposed in [81]. It was shown that the proposed mathematical procedures allow determining the order parameters P_{20} and P_{40} for liquid crystal materials with accuracy comparable to Raman spectroscopy and nuclear magnetic resonance. Recently, improvements of the experimental setup made possible in situ monitoring of structural changes by rapid recording of XRD images [85, 86].

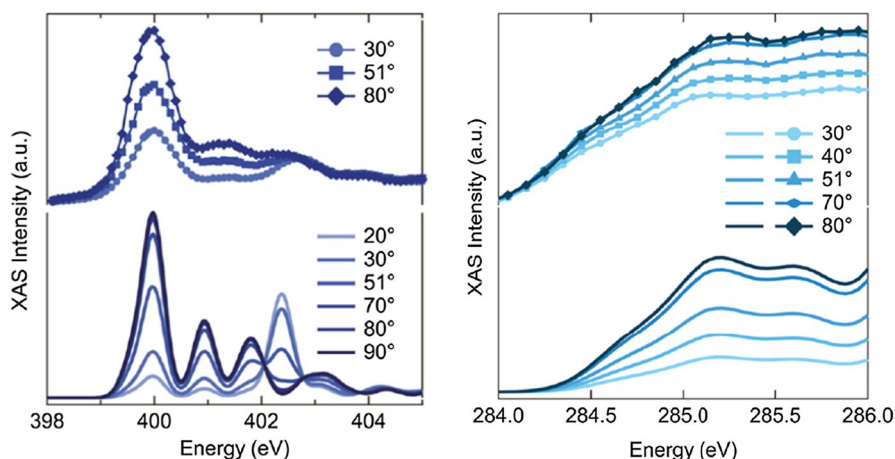


Fig. 4 Experimental (symbol with line) and simulated (line) angle-dependent data for the nitrogen and carbon K -edges of orientationally ordered polythiophene. Reproduced from [71] (<https://pubs.acs.org/doi/10.1021/acs.jpcc.7b01353>) with permission of ACS. Further permissions related to the material excerpted should be directed to the ACS

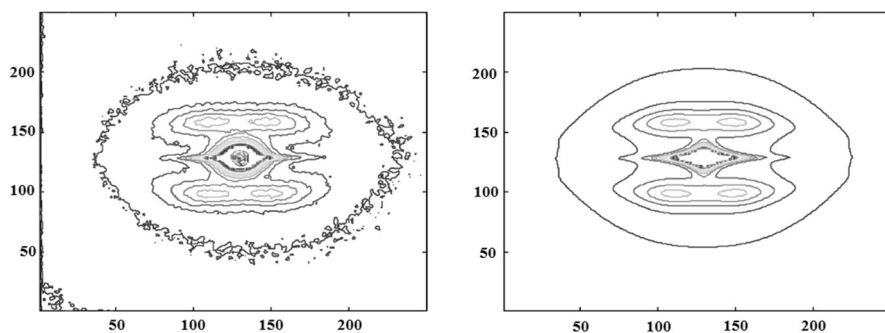


Fig. 5 Diffraction pattern of nylon 6 fiber (left) and the result of its simulation (right). Reproduced from [84] with permission of Rigaku

5 Magnetic Resonance

Both in the case of EPR and NMR, the resonance conditions depend on the orientation of studied molecule relative to the direction of magnetic field. Therefore, the signals of the molecules with different orientations are observed in the spectrum on different positions. This feature is the basis of qualitative advantage of magnetic resonance in comparison with other experimental technique for study of the orientational ordering. Indeed, in the case of optical and NEXAFS methods the signals caused by the molecules with different orientations have coincident positions and differ only in intensity. In the case of magnetic resonance, the signals of the molecules with different orientations do not coincide, so change of the orientation of anisotropic sample relative the magnetic field leads to change of the spectrum shape. For this reason, there is no theoretical limit for determination of high rank order parameters from the magnetic resonance spectra. Should the components of EPR and NMR spectra be infinitely narrow, the analysis of the spectra would provide order parameters of any rank. In practice, the rank of determined order parameters is limited by broadening of spectral lines, superposition of components, experimental noise etc.

5.1 Nuclear Magnetic Resonance

The resonance conditions in NMR are defined by a few factors: chemical shift σ , spin–spin, dipole–dipole and quadrupole interactions. The chemical shift depends on the orientation of screening molecular orbitals with respect to the external magnetic field. Anisotropy of chemical shift is described by a second-rank tensor with nonzero trace. The molecular rotations in liquid solution average anisotropy of chemical shift. The principal axes of chemical shift tensor are determined by the spatial location of molecular orbitals and depend on the symmetry of molecular fragment considered. The principal axes for many molecular fragments are accurately determined [87, 88]. Figure 6 shows ^{13}C NMR spectra of deformed

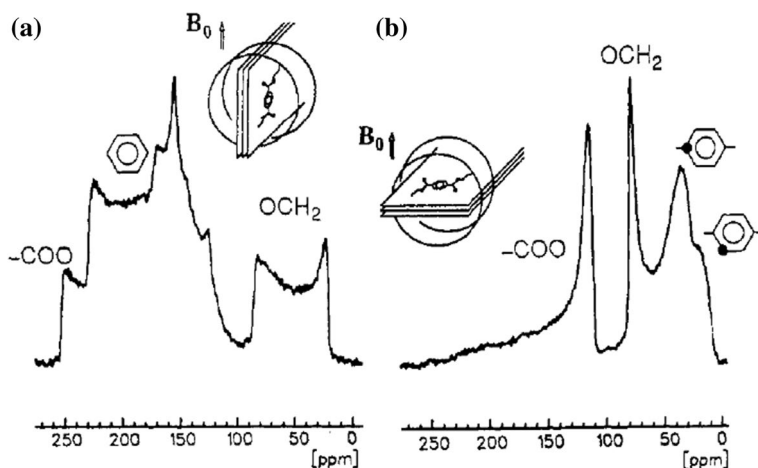


Fig. 6 1D static ^{13}C NMR spectra for a biaxially drawn 12- μm PET film recorded at different orientations of the sample in magnetic field. Reproduced from [89] with permission of ACS

polyethylene terephthalate film recorded at different orientations of the sample relative to magnetic field [89].

The spin–spin and dipole–dipole interactions of magnetic nuclei are also described by the second-rank tensors [J] and [D], respectively. Tensor [D] in contrast to tensor [J] has zero trace. The first-order quadrupole interaction is described by the second-rank tensor similar to chemical shift and spin–spin interaction. The second-order quadrupole interaction cannot be described by the second-rank tensor.

The contribution of various interactions to the shape of spectrum differs significantly for different systems. The anisotropy of nuclear magnetic interactions leads to significant broadening of the NMR spectra of solids. NMR spectra are generally used for determination of chemical structure of the studied substance. In this case the anisotropy is averaged by rotation of sample around an axis of 54.74° to magnetic field (the magic angle of the second Legendre polynomial) with frequency slightly larger than the line broadening caused by anisotropic magnetic interactions. This method, called MAS (magic angle spinning), leads to averaging of chemical shifts, spin–spin and the first-order quadrupole interactions, and vanishes the dipole–dipole broadening. To average the second-order quadrupole interactions dependent also on the fourth Legendre polynomial it is necessary to rotate the sample around the axes of 30.55° or 70.12° (magic angles of the fourth Legendre polynomial). The corresponding DAS (dynamic angle spinning) and DOR (double rotation) techniques are described in detail in [90]. It will be shown below that the techniques based on the rotation of the sample in a magnetic field can be used for determination of the molecular orientational ordering.

Several methods have been developed to date for determination of the orientational ordering by NMR spectroscopy. The computer program LAOCOONOR, later renamed to SHAPE, was developed for the numerical simulation of NMR spectra of orientationally ordered molecules containing several magnetic nuclei. The program

permits to compare the calculated and experimental spectra and to estimate the order parameters and the parameters of dipole–dipole interaction. Use of this approach for study of order of liquid crystalline substances is described in [91–93]. The first determination of all five elements of the Saupe matrix was presented in [93]. As an illustration, Fig. 7 shows the experimental and calculated NMR spectra of pyridine in ordered nematic liquid crystal [91].

The technique based on computer simulation of nuclear magnetic resonance spectra is not widely used. Probably, the reason is the procedure for comparison of calculated and experimental spectra. This procedure is based on an iterative gradient method suited for description of the shape of spectral components, but very poorly adapted for fitting of their position in spectrum. Indeed, if the components of the calculated and experimental spectra do not coincide, the residual value does not depend on the distance between them. Thus, it is necessary to adjust positions of spectral components manually and only after that to use the minimizer program.

The most prominent progress in the characterization of the orientational order by NMR spectroscopy was achieved by Spiess et al. [88, 89, 94–97]. The developed experimental methods and procedures for the spectral analysis allow determining the order parameters of high (above the 4th) ranks and estimating the characteristics of biaxial molecular ordering. The developed method was also used by other authors (see, for example, [98–100]). As it was shown above, a single spectrum is insufficient for unambiguous determination of the molecular orientational characteristics. Two fundamentally different approaches for overcoming of this problem in the case of NMR spectroscopy were developed: synch-MAS based on the synchronization of sample rotation with data acquisition and the recording of the angular dependence

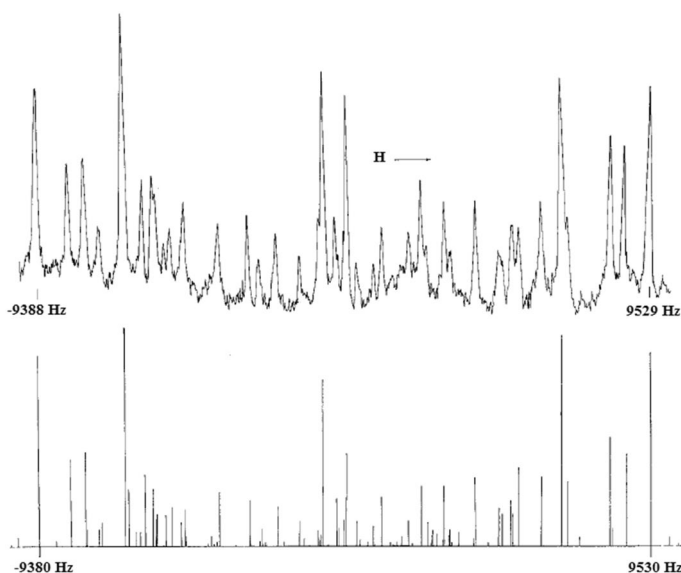


Fig. 7 Observed (up) and calculated (down) NMR spectra of pyridine oriented in the nematic phase of anisole-azophenyl-n-capronate. Reproduced from [91] with permission of Taylor & Francis Ltd

of spectrum for non-rotating sample. Both methods are based on the chemical shift anisotropy and employ the spectral bands of “rare” nuclei— ^2H or ^{13}C .

The synchronized magic angle spinning spectroscopy (synch-MAS or, in earlier works, ROSMAS) consists in synchronizing the rotor phase and the pulse sequence generated the NMR spectrum. The significant contribution of dispersion in the 1D synch-MAS spectra leads to a strong line broadening and significant decrease of informativity of the experiment. Therefore, 2D and 3D experiments are used at present to study orientationally ordered samples. The pulse sequences used for such experiments are described in detail in [88, 97].

Figure 8 shows the calculated 2D synch-MAS spectra of isotropic and orientationally ordered samples [88]. In Fig. 8c, one can see that components at $\omega_1 \neq 0$ are observed in the spectrum in the case of the orientationally ordered sample in contrast to the spectrum for disordered sample shown in Fig. 8a. In the case of the sample with axial symmetry rotated around anisotropy axis (Fig. 8b), the components at $\omega_1 \neq 0$ are negligible, but the amplitudes of the components at $\omega_1 = 0$ differs from the spectrum of disordered sample.

Figure 9a demonstrates the experimental 2D ^{13}C synch-MAS spectra for polyethylene terephthalate fibers [96]. The lines marked as GE, PA, UA and CA correspond to the carbon atoms in different fragments of molecule. Based on these spectra, the distribution functions of the fiber axis orientation were reconstructed in the principal frames of the chemical shift tensors of different C-containing molecular fragments (Fig. 9b, c). The possibility to determine the orientational ordering of various molecular fragments independently is a significant advantage of NMR spectroscopy.

Another way of NMR study of the orientationally ordered systems is DECODER spectroscopy (direction exchange with correlation for orientation distribution evaluation and reconstruction), based on the spectra for non-rotating sample at several fixed positions in a magnetic field. This approach is carried out by turning the sample by a certain angle during the mixing period. The experimental design, as well as the principle of data analysis, is illustrated in Fig. 10. The magnetic field vector B_0 “switches” between the two positions B_{01} and B_{02} in the sample coordinate frame. The frequency coordinates ω_1 and ω_2 of a signal sweep cones in the sample

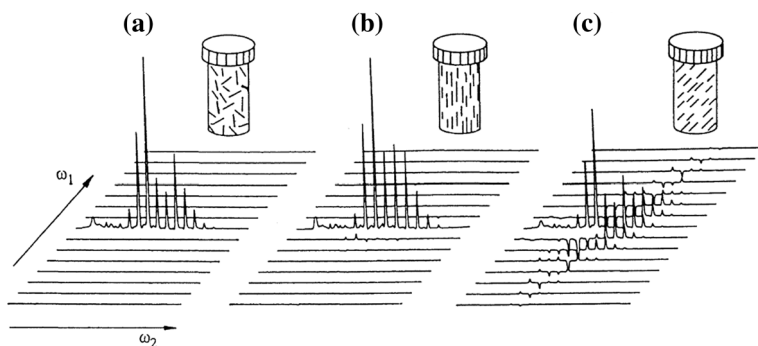


Fig. 8 Calculated 2Dsynch-MAS spectra of isotropic and orientationally ordered samples. The sample rotates around an axis directed along the cylinder. Reproduced from [88] with permission of Elsevier

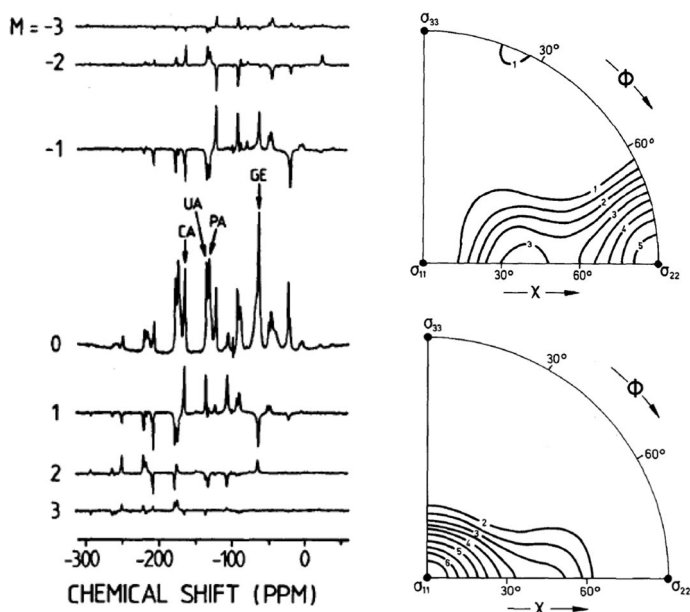


Fig. 9 2D-MAS ^{13}C spectrum of PET fibers, oriented at an angle of $39^\circ \pm 3^\circ$ to the rotor axis, and spinning at 3.2 kHz (GE—glycolic ethylene; PA—aromatic carbon with hydrogen substitute; UA—aromatic carbon without hydrogen substitute; CA—carbonyl) (a); contour plots of the orientation distribution functions of the fiber axis in the frames of the aromatic carbons shielding tensors (b, c). Reproduced from [96] with permission of AIP Publishing

coordinate frame, which can be represented as circles on a sphere of unit radius. The intersection points of the circles define several possible orientations of a given molecular axis relative to the sample. This methodology is close to the method of wide-angle X-ray scattering spectroscopy. The analogies between these methods are considered in detail in [88].

For simplification of the procedure of extracting the values of order parameters it was proposed to represent experimental spectra as a sum of subspectra with coefficients corresponding to the moments of orientation distribution function [88, 95, 98]. The coefficients are selected in such a way that every calculated spectrum would be as close as possible to the experimental one. Obviously, the higher anisotropy of the studied system, the larger number of expansion terms should be used.

If the molecules are oriented mainly in one direction, the procedure for simulation of NMR spectra can be simplified using the distribution in form of Gaussian function. The Gaussian orientation distribution is defined by three parameters describing the direction of orientation axis and the width of distribution. At the same time the distribution can be expanded in a series of spherical functions. For example, the ordering of macromolecules in crystalline domains of stretched deuterated polyethylene was described by order parameters up to rank 8 calculated from the obtained Gaussian distribution [95]. The independent variation of the order parameters, as well as the addition of higher rank parameters did not improve agreement with experimental spectra. The authors concluded that the orientation distribution of

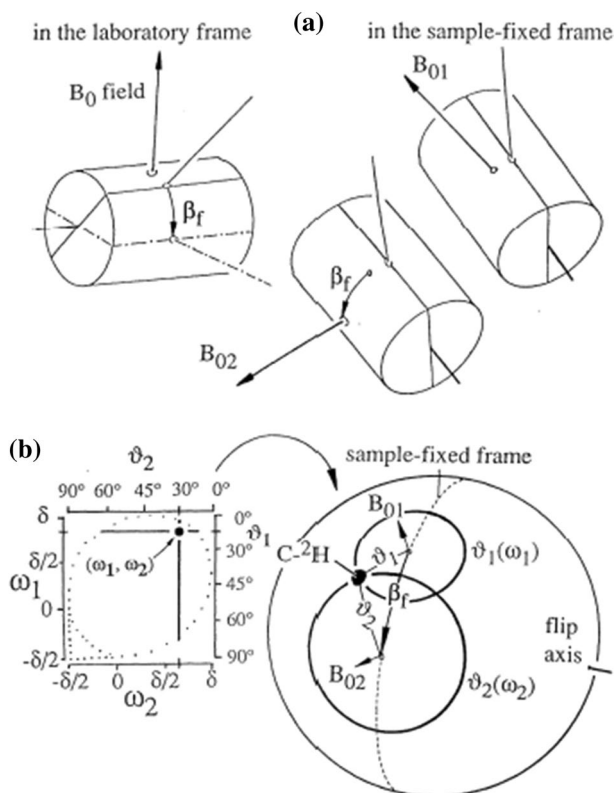


Fig. 10 Experimental design and the principle of data analysis in DECODER. Reproduced from [88] with permission of Elsevier

polymer molecules in stretched polyethylene really has the Gaussian shape. It should be noted that assumption of Gaussian shape for molecular orientation distribution function is not generally correct.

A significant advantage of the described methods is the possibility of determination of high rank order parameters. For example, the orientation of PET macromolecules in fibers, as well as in axial and biaxial films, was described using ^{13}C DECODER spectroscopy with evaluation of the order parameters up to 14th rank [89]. It should be noted that DECODER spectroscopy permits evaluation of the order parameters of higher rank than synch-MAS spectroscopy and, therefore, describes orientational alignment in more details (Table 1).

The synch-MAS and DECODER procedures are complicated both experimentally and theoretically. However, at present time there is no worthy alternative to them. Some researchers proposed methods for determining the molecular orientational ordering from the NMR spectrum of motionless sample. The authors of [101, 102] determined the values of P_{20} for stretched deuterated polybutadiene using computer simulation of a single NMR spectrum. It was shown that degree of polymer

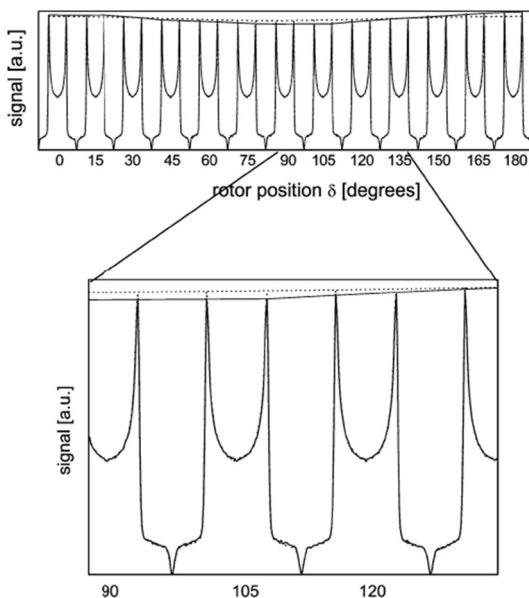
Table 1 Order parameters of PET fibers determined using synch-MAS 2D NMR and DECODER 2D NMR [88]

		P_2	P_4	P_6	P_8	P_{10}
Synch-MAS	OCH ₂	0.55 ± 0.02	0.55 ± 0.03	–	–	–
Synch-MAS	COO	0.51 ± 0.02	0.41 ± 0.06	0.55 ± 0.15	–	–
DECODER	OCH ₂	0.60 ± 0.05	0.47 ± 0.05	0.37 ± 0.05	0.26	0.17

ordering is reflected in the signal splitting and line shape. The authors of [103, 104] proposed a joint numerical simulations of series of NMR spectra recorded at different orientations of axial sample relative to magnetic field as an alternative to DECODER spectroscopy. Figure 11 presents set of spectra of compressed deuterated polymethyl methacrylate. The spectra were recorded at discrete orientations of the sample with the step of 15° around an axis perpendicular to the deformation direction. Information on the molecular ordering is contained in the shape of curves connecting the spectral maxima. The order parameters P_{20} , P_{22} , P_{40} , P_{42} , P_{44} , and P_{60} were determined from the presented experimental data. The reconstruction of orientation distribution became possible with use comprehensive regularization procedures. The choice of the regularization scheme was shown to be critical. In our opinion, the reliability of obtained values is not high. To date, the proposed method has not been used by other researchers.

The additional factors influencing the shape of NMR spectra are the rotation of molecules as a whole and the intramolecular rotation of molecular fragments. Discrimination of the sample domains with higher and lower molecular mobility can

Fig. 11 Set of 13 experimental 1D quadrupolar solid state NMR spectra of PMMA strained below the glass transition temperature; the envelopes of two series of experimental spectra for samples with different deformation are presented in the top as solid and dotted lines. Reproduced from [103] with permission of ACS



be done based on the line width of NMR signal. For example, the signals of amorphous and crystalline domains of polymer were distinguished in [95, 98, 105]. The influence of molecular rotational mobility on the line shape of magnetic resonance spectrum was considered theoretically in [106]. Two types of rotation were considered: “liquid-like” rotation (Brownian rotational diffusion), “solid-like” rotation (rotational jumps on a certain angle) and their combination. It was shown that these two types of rotational mobility cause different changes of the spectral line. In particular, high Brownian diffusion rate leads to the Lorentzian shape of line. When the liquid-like rotation slows down and the frequency of jumps increases, the line narrows and the line shape deviates from the Lorentzian function. It should be noted that the mathematical consideration presented in [106] is applicable to both NMR and EPR spectra.

The shape of the NMR spectral line at various frequencies of rotational jumps was calculated in [107]. Attempt of simultaneous characterization of the rotational mobility and the molecular orientational ordering by ^{13}C synch-MAS NMR spectra of highly ordered crystalline polyformaldehyde is described in [108, 109]. The authors asserted that the best simulation of experimental spectra was achieved in the case of “solid-like” rotational mobility with rotation angle of $\pm 200^\circ$. However, the procedure for determination of the optimal rotation angle, as well as uncertainty of the obtained value was not discussed. In general, it should be concluded that the simultaneous determination of the rotational mobility and the orientational ordering by NMR spectroscopy at present is the unsolved problem.

It is necessary to consider in more detail the potential of NMR spectroscopy in characterization of the molecular orientational ordering in liquid crystals. Obviously, DECODER and synch-MAS techniques requiring sample rotation cannot be used to study liquid substances. In addition, the rotational molecular mobility in liquid crystals with typical correlation time $\sim 10^{-9}$ s leads to averaging of the most part of magnetic anisotropy [110]. The ^2H NMR is the best method for studying liquid crystals at the present time. Deuterium nucleus has a spin equal to unity and demonstrates a quadrupole moment interacting with a gradient of the local electric field. Rapid stochastic molecular rotations in ordinary liquids average the anisotropy of the quadrupole tensor to zero, and corresponding NMR signal becomes a single line. In the orientationally ordered phase, in contrary, the signal consists of two lines of equal intensity. The distance between the lines is defined by the quadrupole tensor and the molecular orientation. When deuterium nucleus is located in the aliphatic fragment, the quadrupole tensor has almost axial anisotropy with the axis directed along the C–D bond. The quadrupole splitting then is determined by the angle between the C–D axis and the direction of magnetic field [111]:

$$\Delta\nu = \Delta\nu_0(3 \cos^2 \theta - 1)/2 \quad (9a)$$

$$\Delta\nu_0 = (3/2)q_{CD}S_{CD}, \quad (9b)$$

where q_{CD} is the constant of the quadrupole interaction; S_{CD} is the second-rank order parameter of the C–D axis. The works [111–115] are devoted to consideration of the angular dependences of the quadrupole splitting for deuterated nematic 5CB liquid

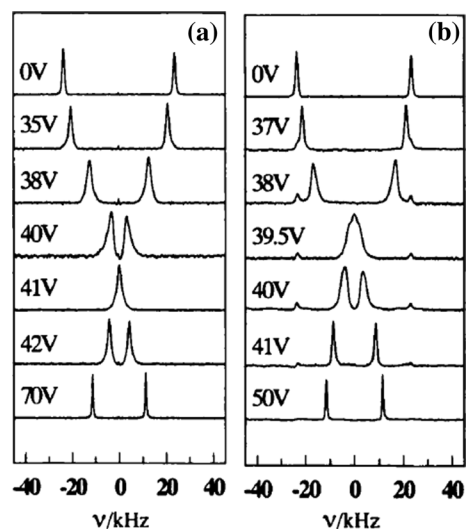
crystalline phase as well as nematic and smectic 8CB phases. The liquid crystalline samples oriented between two glass plates were reoriented by electric field to measure specific time of the molecular reorientation. Change in the quadrupole splitting of the NMR spectra was used for monitoring the reorientation process (Fig. 12). As a result of these experiments, the values of relaxation times, the coefficients of rotational viscosity and the diamagnetic anisotropy were determined. The molecular orientational ordering was considered only qualitatively. For example, Fig. 12 was commented by the authors of [111] as follows: “it can be seen that with a strong orienting action of the surface, a small but noticeable fraction is present in the sample, in which the director is still oriented to a greater or lesser extent parallel to the surface of the glass plates”.

The data presented in this section allow concluding that nuclear magnetic resonance is a powerful method for characterization of the molecular orientational ordering. NMR has no theoretical restrictions on determining the order parameters of high ranks, as well as on establishing the characteristics of biaxially ordered systems. A significant advantage of this method is the possibility of an independent specification of the ordering of various molecular fragments [116]. Nevertheless, it should be recognized that the NMR methods developed to date cannot be applied to many objects. Further development is necessary for application of NMR for study of ordered soft materials.

5.2 Electron Paramagnetic Resonance

In the case of electron paramagnetic resonance, like the nuclear magnetic resonance, there is no theoretical limit for determination of high rank orientational moments. The limitations in this case are defined by width of the individual resonance line, by overlapping of the spectral components and by quality of spectra recording.

Fig. 12 Deuterium NMR spectra of 5CB-d2 liquid crystal measured at various applied electric field for two nematic cells: (a) 55.7 μm cell with weak anchoring condition and (b) 55.5 μm with strong anchoring condition. Reproduced from [111] with permission of Taylor & Francis Ltd



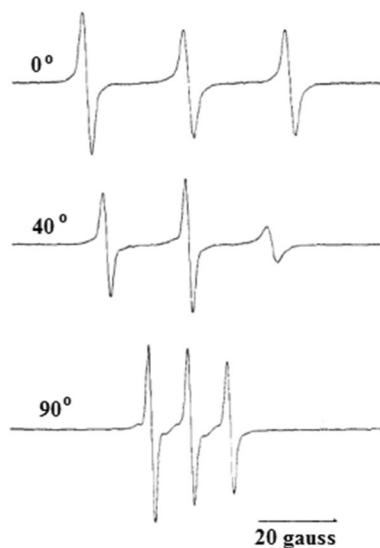
The main characteristics of paramagnetic particles determining the resonance condition are known to be the gyromagnetic ratio (g -factor) and the constants of hyperfine interaction (hfi). Both the g -factor and hfi constants are the second-rank tensors with nonzero traces. The principal axes of the g - and hfi-tensors in the molecular frame are known for many radicals.

Since most substances and materials are not paramagnetic the methods of spin probe and spin label are widely used [117]. The most common spin probes are stable nitroxide radicals which are characterized by high stability and large anisotropy of hyperfine interaction. The large anisotropy makes the EPR spectra of nitroxides sensitive to the rotational mobility and the orientational ordering of paramagnetic molecules.

In the first works devoted to determination of the molecular orientational ordering by EPR spectroscopy, the order parameter P_{20} was estimated using the angular dependence of the parallel hyperfine component of vanadylacetylacetonate in liquid crystalline medium [118]. It was assumed that the amplitude of this component is proportional to the number of molecules oriented along magnetic field. Later in [119, 120] it was theoretically shown that the higher the molecular ordering the greater is the difference between the orientation distribution function obtained in this way and the true function. Another significant weakness of the method is the using only one specific point of spectrum, thus large part of spectral information concerning the molecular orientational ordering is lost.

A numerical treatment of EPR spectra of spin probes in liquid crystalline media were developed in a series of works by McFarland, McConnell, Luckhurst and Zannoni [121–126]. The used procedures were intended for consideration of spectra in the fast rotating regime when the molecular rotation correlation time is in the range $1 \cdot 10^{-9}$ – $5 \cdot 10^{-11}$ s. Spectra of nitroxide radicals in this condition consist of three well-resolved components (Fig. 13). The half-width of the spectrum lines is determined

Fig. 13 EPR spectra for the 5-doxyl stearic acid probe in lamellar G phase for three orientations of director relative to magnetic field. Reproduced from [124] with permission of Taylor & Francis Ltd




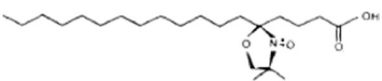
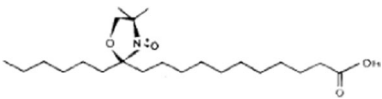
by the spin–spin relaxation rate and can be described in the terms of the Redfield theory [127] as follows:

$$1/T_2(m) = A(\gamma) + B(\gamma) \cdot m + C(\gamma) \cdot m^2 + X(\gamma), \quad (10)$$

where T_2 is the time of spin–spin relaxation, m is the projection of the nitrogen nucleus spin on the direction of external magnetic field, A , B , C are constants depending on the magnetic parameters, X is the contribution independent on the rotation mobility, γ is the angle between the director of liquid crystal and the direction of magnetic field. The last term in the expression (10) is caused by unresolved proton hyperfine structure. As the experimental EPR spectrum is the sum of spectra of radicals with different orientations relative to magnetic field, it is clear, that the shape of the spectrum contains information about the molecular orientation distribution.

The authors of [121–126] used large elongated nitroxide radicals (3-doxyl-5 α -cholestane, 5- and 12-doxylstearic acids) as spin probes. The rotational diffusion of these molecules in liquid crystalline media is approximately axial. The orthorhombic anisotropy of the magnetic parameters in these conditions is averaged to the effective axial parameters $-\tilde{g}_\perp, \tilde{g}_\parallel, \tilde{A}_\perp, \tilde{A}_\parallel$. It was shown that the order parameter P_{20} in this case can be determined from the positions of the high-field and low-field components of the spectrum. The angular dependence of the coefficients A , B , C

Table 2 Values of the orientational order parameters for radicals in smectic liquid crystal estimated from angular dependences of the coefficients B , C (averaging for B and C) and calculated according to the Maier–Saupe theory [124]

	P_{20} experiment	P_{40} experiment	P_{40} calculation by Maier–Saupe theory
 (I)	0.76	0.43	0.43
 (II)	0.61	0.11	0.25
 (III)	0.23	-0.08	0.04

permits to determine the order parameter P_{40} and the molecular rotational correlation times τ_\parallel and τ_\perp . It should be noted that parameter A , in contrast to the parameters B and C , includes the contribution of the unresolved hyperfine structure; therefore, as a rule, the angular dependence of the B and C is used for determination of the rotation parameters and the orientational characteristics.

Table 2 presents the values of order parameters P_{20} and P_{40} for spin probes in the smectic liquid crystalline phase. The parameters obtained from angular dependences of the coefficients B and C are compared with the values calculated within the Maier–Saupe theory [128]. It is seen that in the case of the rigid radical I these values agree, while for flexible probes II and III, the experimentally determined orientational moments contradict to the theoretically predicted. Thus, a single Maier–Saupe potential is insufficient for correct description of flexible spin probes.

The described method has serious limitations. The method was worked out only for study of axial samples. Samples with more sophisticated ordering cannot be analyzed in this way. The orientational ordering in this method is described by order parameters of the second and fourth ranks only. The determination of orientational moments of the higher ranks is not possible. In addition, the rotation of spin probes is assumed to be axial, and therefore, this approach can be applied only for elongated paramagnetic molecules. It is not applicable in the case of small compact spin probes. And most importantly, the proposed method is based on Redfield theory and thus can only be applied to EPR spectra in the range of fast rotations. Since liquid crystals are viscous solvents, in practice this condition is rarely realized.

Ovchinnikov et al. [129, 130] proposed the “express analysis” (the authors’ term) of EPR spectra of the orientationally ordered samples. The method is based on modeling of the angular dependences for intensities of spectrum singular points corresponding to the canonical magnetic axes of paramagnetic molecules. Corresponding mathematical tools was developed for axial systems and was applied for the transition metal complexes oriented in liquid crystals. The orientation distribution function was assumed to be as follows:

$$P(\theta_x, \theta_y, \theta_z) = N \cdot \exp(-a_x \cos^2 \theta_x - a_y \cos^2 \theta_y - a_z \cos^2 \theta_z), \quad (11)$$

where N is the normalization factor; $\cos \theta_i$ are the direction cosines of the symmetry axis (director of the liquid crystal) in the molecular coordinate frame (x, y, z) ; a_i are the distribution parameters.

The joint computer simulation of a series of EPR spectra of an anisotropic sample recorded at different sample orientations in magnetic field was used in the works of Boguslavsky et al. [131, 132]. The angular dependence of all points of the spectrum is used in this case. The molecular orientation distribution in these works is presented as three independent Gaussian distribution corresponding to three Euler angles (ψ, ω, φ) connecting the molecular frame with the sample frame, as follows:

$$P(\psi, \omega, \varphi) = P(\psi)P(\omega)P(\varphi) = \exp \left[-\ln 2 \frac{(\psi - \psi_m)^2}{\sigma_\psi^2} \right] \exp \left[-\ln 2 \frac{(\omega - \omega_m)^2}{\sigma_\omega^2} \right] \exp \left[-\ln 2 \frac{(\varphi - \varphi_m)^2}{\sigma_\varphi^2} \right], \quad (12)$$

where $(\psi_m, \omega_m, \varphi_m)$ are the Euler angles of predominant molecular orientation in the sample, σ_i are the width of distributions on (ψ, ω, φ) angles assumed to be independent.

The method was tested for the axial samples of copper (II) dipivaloylmethanate films. It is clear that the distribution (12) described by only three independent parameters cannot be used for the independent estimation of the high rank order parameters.

The widely used method for description of the orientational ordering of paramagnetic molecules was developed by Freed and el. [133–137]. The method is based on the joint simulation of the spectra recorded at different orientations of the sample in magnetic field. The minimization procedure is used for spectral fitting. The orientation distribution of spin probes in the framework of this method is considered to be dictated by an averaged ordering potential of the medium. This approach is called the mean field potential method (MF). The orienting potential $U(\theta, \varphi)$ is expressed as a series of spherical functions of the second and fourth ranks:

$$\frac{U(\beta, \gamma)}{k_b T} = - \sum_{j,m} c_{j,m} D_{0m}^j(\beta, \gamma), \quad (13)$$

where D_{0m}^j are the Wigner functions; angles β, γ determine the local director in the coordinate frame of paramagnetic molecule; the parameters $c_{j,m}$ are expressed in units of $k_b T$.

The orientation distribution function is presented as follows:

$$\rho(\beta, \gamma) = \frac{e^{-U(\beta, \gamma)/k_b T}}{\int e^{-U(\beta, \gamma)/k_b T} \sin \beta \cdot d\beta \cdot d\gamma}. \quad (14)$$

Obviously, this approach is intended for study of the systems in Maxwell–Boltzmann equilibrium. The stochastic Liouville equation is used for calculation of the slow motional EPR spectra corresponding to the rotational correlation times 10^{-7} – 10^{-9} s. The most detailed discussion of the method, including theoretical basis, description of the software and examples of application is presented in [133–135].

The described method is applicable for description of the EPR spectra recorded at different frequencies. Joint analysis of the X- and W- band EPR spectra was presented in [136]. The mobility of nitroxyl labeled T4 lysozyme in the solution at the temperatures 275–305 K was studied by EPR with frequencies of 9, 95, 170, and 240 GHz [137].

The mean field potential method approves itself as a powerful tool for interpretation of the EPR spectra of rotated spin probes in ordered media. Limitations of this approach were analyzed in [138]. The most important one is a *priory* postulation of the same orientation distribution in all points of a sample. Both independent determination of the high rank order parameters and the correct consideration of real structure of the material with different local ordering became impossible as a result of this postulation. The impossibility of independent measurement of the order parameters impedes to revelation of sophisticated features of orientation distribution.

The simplest and, at the same time, accurate approach to determining the orientational ordering of paramagnetic molecules using EPR spectra was proposed by Burghardt et al. [139–142]. The works of these authors were devoted to study of the orientation distribution of the muscle myosin labeled by nitroxide moiety. The orientation distribution of the paramagnetic fragments was determined by joint simulation of the spectra recorded at different orientations of the sample in magnetic field as in the case of MF method. But according to the procedure of Burghardt et al. the orientation distribution function was expressed by Eq. (2) as a series of spherical functions. The coefficients of Eq. (2) were chosen to achieve the best coincidence of calculated and experimental spectra. To determine the maximum rank of orientation moments, the spectral simulation must be performed many times with successively increasing the rank of decomposition. The procedure is completed when the addition of the higher rank spherical functions was not reducing the difference between the experimental and theoretically calculated spectra. This approach is not based on any assumptions and presumes determination of the orientational ordering “as it is”. The authors fairly call this approach as “model-free”. A serious limitation is negligible rotation mobility of paramagnetic moiety (rigid limit condition) necessary for this method. Besides, the method was applied to study a single system only.

The authors of the present review have shown that the approach of Burghardt et al. can be applied for determination of the orientation ordering of various paramagnetic molecules in different matrices: super-cooled liquid crystals [143–146], stretched polymers [147–149], super-cooled glasses [150, 151], graphite oxide membranes [152]. The obtained results showed that fitting of the angular dependence of the rigid limit EPR spectra leads to determination of the order parameters up to rank 10 [146]. The values of order parameters obtained by EPR spectroscopy were found to agree with the results of optical measurements [145, 151]. The developed software for simulation of rigid limit EPR spectra and determination of order parameters by fitting are available for free use (<http://www.chem.msu.ru/eng/lab/chemkin/ODF3/>).

Further development of this approach is the additional possibility to take into consideration the rotation mobility of molecules in ordered medium. This aim has been achieved by the simultaneous independent description of local orientational potential by expressions (Eqs. 13, 14) and the distribution of the local director in the sample by expression (Eq. 1). The rotation mobility of the spin probe in the

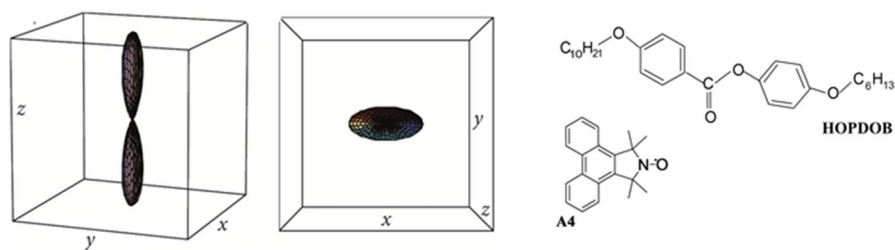


Fig. 14 Orientational distribution of local director of liquid crystal HOPDOB in molecular coordinate frame of spin probe A4

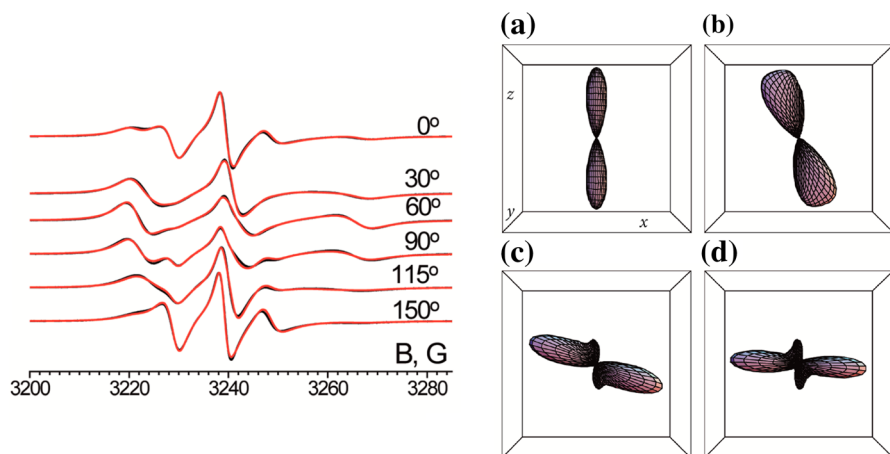


Fig. 15 Angular dependence of the EPR spectra of a nitroxide radical in a non-orthorhombic liquid crystal (8CB, 297 K, SmA) prepared at 1.2 T (see text). Black lines are experimental spectra; red lines are the results of numerical simulation. Orientation distribution functions corresponding to magnetic field 0T (a), 0.9T (b), 1.2T (c), 1.47T (d). Reproduced from [153] with permission of ACS

local potential is described by the stochastic Liouville equation. The high frequency librations partially averaging the radical magnetic parameters can be also taken into account. This combined model is realized as the computer program available for free use (<https://sourceforge.net/projects/odfr/>). The method was used for determination of the orientational characteristics for mesophases of liquid crystals [145, 153] and liquid crystalline polymers [147–149]. The described combined method was also used in the case of the biradical spin probes containing two nitroxide fragments in the structure of molecule [154, 155]. The orientation-dependent dipole–dipole interaction of nitroxide fragments is an additional source of information in this case. The corresponding software also available (<https://sourceforge.net/projects/orthos-epr/>).

The order parameters up to rank 18 were estimated for the best aligned liquid crystalline media. The parameters of molecular rotations were determined at once [153]. It was revealed that the local ordering of additive molecules in the axial liquid crystals is commonly not axial. The example of a typical molecular biaxiality is shown in Fig. 14.

The discussed method was found to be applicable for characterization of the molecular orientational order of low symmetry. Figure 15 demonstrates the EPR spectra and the orientation distribution functions of nitroxide in the liquid crystal subjected by two differently directed orienting influences: the hydrophobic surfaces and the magnetic field. It is seen that the spectra recorded at the angles of 30° and 150° between the sample normal and the magnetic field differ significantly, thus, the sample is non-orthorhombic. The orientation distribution functions corresponding to the different magnetic field show that the part of the liquid crystalline sample retains the initial orientation dictated by hydrophobic surfaces and other part forms the smectic structure with director turned relative to both surface and magnetic field.

Table 3 Characteristics of methods used for study of molecular orientational ordering

Method	Rank ODF (theory)	Rank ODF (real)	Time resolution	Selectivity ^a
Birefringence	2	2	Nanoseconds [14]	No
IR	2	2	Sub-milliseconds [33]	Yes
UV/Vis	2	2	Picoseconds [157]	Yes
Fluorescence	4	2–4	Picoseconds [158]	No
Raman	4	2–4	Picoseconds [159]	Yes
NEXAFS	2	2	Picoseconds [160] ^b	Yes
XRD	∞	2–4	Seconds [86]	No
NMR	∞	16	Dozens of hours [97]	Yes
EPR	∞	18	100 ms [149]	No

^aBy selectivity we mean the possibility of determining the ordering of various fragments of a molecule

^bThe cited work is not devoted to the study of orientational ordering

In general, it can be concluded that EPR spectroscopy at present is the most powerful and informative method for characterization of the orientation distribution of molecules in aligned samples. The developed experimental and numerical techniques are capable to elucidate subtle features of the orientation distribution function. The limitation of EPR is a “global” character of the obtained data, hampering the determination of spatial variation of properties in studied samples. In principle, this drawback can be overcome to some extent by introducing different radicals into different parts of the sample. For example, the authors of [156] studying the stretched polyethylene have used the nitroxide probe introduced into the amorphous phase and the alkyl radicals generated in the crystalline domains to compare the orientation order. Another significant weakness of the continuous wave EPR is the poor time resolution making impossible study of fast evolution of orientation distribution. It is necessary to note that modern Bruker spectrometers are equipped with the Rapid Scan function for recording the EPR spectrum with a time resolution of 10 μ s. An alternative approach to EPR determination of rapid changes of orientational order was employed in paper [149] to study fast reorientation of liquid crystals in the magnetic field. In this work, the recording of full EPR spectra at distinct moments of time was replaced by recording of time dependences of EPR signal at different values of magnetic field. This technique was used to monitor the change of EPR spectrum due to liquid crystal reorientation with time resolution of 100 ms.

6 Conclusion

At present, there are several experimental techniques appropriate for monitoring of the molecular orientational ordering. The choice of a suitable method depends on the properties of material studied and on purpose of the study. The comparison of the capabilities of various methods is given in Table 3.

A comparison of orientational ordering of materials under the various influences is commonly carried out using optical methods. The advantage of optical methods is the possibility of monitoring the fast ordering/disordering processes in real-time. The optical determination of the order parameters of second rank can be performed with minimum financial and labor costs. The methods for detailed determination of molecular orientation distribution are nuclear magnetic resonance and electron paramagnetic resonance. The position of the resonance NMR or EPR signals depends on the orientation of the molecule relative to magnetic field direction. This fact significantly increases the informativity of magnetic resonance in comparison with other experimental methods. From the point of view of the experimental design, EPR spectroscopy is preferential comparative to NMR, since it does not require rapid rotation of the sample. For this reason, EPR can be used to study of soft matter, for example, liquid crystals and biological tissues. One can also note the relative simplicity and low cost of EPR experiments in comparison with NMR experiments. Currently available methods for recording and numerical treatment of angular dependence of EPR spectra are appropriate to determine the high ranks order parameters of mobile paramagnetic molecules in samples of arbitrary symmetry.

Acknowledgements This work was supported by the RFBR (Grant 18-29-19120 mk).

References

1. Zannoni C., in *The Molecular Physics of Liquid Crystals*, ed. by Luckhurst G.R., Gray G.W. (Academic Press, London, 1979), pp. 51–83
2. M. Van Gorp, *Colloid Polym. Sci.* **273**, 607–625 (1995)
3. *Biaxial Nematic Liquid Crystals. Theory, Simulation and Experiment*, ed. by Luckhurst G.R., Sluckin T.J. (Wiley, Chichester, 2015), 383 p
4. Cole K. C., Ajji A. in *Solid Phase Processing of Polymers*, ed. by Ward I. M., Coates Ph. D., Dumoulin M. M. (Hanser Publishers, Munich, 2000), pp. 33–84
5. A.K. Oultache, X. Kong, Ch. Pellerin, J. Brisson, M. Pezolet, R.E. Prudhomme, *Polymer* **42**, 9051–9058 (2001)
6. M.C. Cetinkaya, S. Yildiz, H. Ozbek, P. Losada-Perez, J. Leys, J. Thoen, *Phys. Rev. E* **88**, 042502 (2013)
7. B. Zywucki, W. Kuczynski, G. Czechowski, *Proc. SPIE–Int. Soc. Opt. Eng.* **2372**, 151–156 (1995)
8. J.H. Dumbleton, *J. Polym. Sci. A-2* **6**, 795–800 (1968)
9. S. Rhee, J.L. White, *Polymer* **43**, 5903–5914 (2002)
10. L. Bokobza, *Polymer* **42**, 5415–5423 (2001)
11. S. Sasaki, Y. Sasaki, A. Takahara, T. Kajiyama, *Polymer* **43**, 3441–3446 (2002)
12. O. Yaroschuk, T. Sergan, J. Lindau, S.N. Lee, J. Kelly, L.-C. Chien, *J. Chem Phys.* **114**, 5330–5337 (2001)
13. B.L. Van Horn, H.H. Winter, *Macromolecules* **36**, 8513–8521 (2003)
14. R. Hildebrandt et al., *Phys. Rev. Lett.* **81**, 5548–5551 (1998)
15. A.E. Grishchenko, A.N. Cherkasov, *Phys. Usp.* **40**, 257–272 (1997)
16. L. Hardy, I. Stevenson, A.M. Voice, I.M. Ward, *Polymer* **43**, 6013–6017 (2002)
17. Xu Yiran Zhou, Xiaoyuan Hu Han, Xu Lianghua, Cao Weiyu, *High Performance Polymers* **29**, 1158–1164 (2017)
18. M. Mizushima, T. Kawamura, K. Takahashi, K. Nitta, *e-Polymers*, 068 (2012)
19. T.R. Manley, D.A. Williams, *J. Polymer Sci.* **22**, 1009–1018 (1969)
20. N. Vasantan, *Appl. Spectrosc.* **59**, 897–903 (2005)
21. L.J. Fina, *Appl. Spectrosc. Rev.* **29**, 309–365 (1994)

22. N.J. Clayden, J.G. Eaves, L. Croot, *Polymer* **38**, 159–163 (1997)
23. T. Elsein, M. Brogly, J. Schultz, *Polymer* **44**, 3649–3660 (2003)
24. L.J. Fina, G. Chen, *J. Appl. Polym. Sci.* **48**, 1229–1240 (1993)
25. K.C. Cole, J. Guèvremont, A. Ajji, *Appl. Spectrosc.* **48**, 1513–1521 (1994)
26. J. Guevremont, A. Ajji, K.C. Cole, *Polymer* **36**, 3385–3392 (1995)
27. R. Mendelsohn, G. Mao, C.R. Flach, *Biochimica and Biophysica Acta* **1798**, 788–800 (2010)
28. A. Banc, B. Desbat, D. Renard, Y. Popineau, C. Mangavel, L. Navailles, *Langmuir* **23**, 13066–13075 (2007)
29. M. Gliboff et al., *Langmuir* **29**, 2166–2174 (2013)
30. T. Buffeteau, B. Desbat, S. Besbes, M. Nafati, L. Bokobza, *Polymer* **35**, 2538–2541 (1994)
31. T. Buffeteau, B. Desbat, J.M. Turllet, *Appl. Spectrosc.* **45**, 380–389 (1991)
32. B. Farbos, D. Mauran, Ch. Pellerin, *Vib. Spectrosc.* **51**, 34–38 (2009)
33. S.V. Shilov, H. Skupin, F. Kremer, E. Gebhard, R. Zentel, *Liq. Cryst.* **22**, 203–210 (1997)
34. J. Schellman, H.P. Jensen, *Chem. Rev.* **87**, 1359–1399 (1987)
35. J. Michl, E.W. Thulstrup, *Acc. Chem. Rev.* **20**, 192–199 (1987)
36. D. Bauman, C. Killet, S.E. Boiadjiev, D.A. Lightner, A. Schonhofer, H.-G. Kuball, *J. Phys. Chem.* **100**, 11546–11558 (1996)
37. D. Bauman, H.-G. Kuball, *Chem. Phys.* **176**, 221–231 (1993)
38. M.T. Sims, L.C. Abbott, S.J. Cowling, J.W. Goodby, J.N. Moore, *Chem. Eur. J.* **21**, 10123–10130 (2015)
39. C. Plosceanu, *J. Optoelectr. Adv. Mat.* **4**, 67–72 (2002)
40. A. Ranjkesh, J.-Ch. Choi, K.-I. Joo, H.-W. Park, M.S. Zakerhamidi, H.-R. Kim, *Mol. Cryst. Liq. Cryst.* **647**, 107–118 (2017)
41. A. Rodger, J. Rajendra, R. Murrington et al., *Phys. Chem. Chem. Phys.* **4**, 4051–4057 (2002)
42. S. Kawato, K. Kinoshita Jr, A. Ikegami, *Biochem.* **16**, 2319–2324 (1977)
43. I.N. Dozov, I.I. Penchev, *J. Luminescence* **22**, 69–78 (1980)
44. M.A.R.B. Castanho, S. Lopes, M. Fernandes, *Spectroscopy* **17**, 377–398 (2003)
45. A. Rodger, G. Dorrington, D.L. Ang, *Analyst.* **141**, 6490–6498 (2016)
46. B.M. Bulheller et al., *J. Am. Chem. Soc.* **131**, 13305–13314 (2009)
47. J. Rajendra, M. Baxendale, L.G.D. Rap, A. Rodger, *J. Am. Chem. Soc.* **126**, 11182–11188 (2004)
48. B.A. Clack, D.M. Gray, *Biopolymers* **32**, 795–810 (1992)
49. T. Damerau, M. Hennecke, *J. Chem. Phys.* **103**, 6232–6240 (1995)
50. R.P.H. Kooyman, M.H. Vos, Y.K. Levine, *Chem. Phys.* **81**, 461–472 (1983)
51. P. Lapersonne, J.F. Tassin, P. Sergot, L. Monnerie, G. LeBourvellec, *Polymer* **30**, 1558–1564 (1990)
52. S. Lopes, M.A.R.B. Castanho, *J. Phys. Chem. B* **106**, 7278–7282 (2002)
53. J.B. Faisant de Champchesnel, J.F. Tassin, L. Monnerie, P. Sergot, G. Lorentz, *Polymer* **38**, 4165–4173 (1997)
54. S. Murase, M. Hirami, Y. Nishio, M. Yamamoto, *Polymer* **38**, 4577–4585 (1997)
55. J.H. Nobbs, D.I. Bower, I.M. Ward, *J. Polym. Sci. Polym. Phys.* **17**, 259–272 (1979)
56. M. Levitus, J.L. Bourdelande, G. Marques, P.F. Aramendia, *Photochem. Photobiol. A Chem.* **126**, 77–82 (1999)
57. K.D. Weston, L.S. Goldner, *J. Phys. Chem. B* **105**, 3453–3462 (2001)
58. Monge E.M., Armoogun D.A., Bain A.J., *Proc. of SPIE—The International Society for Optical Engineering*, **4797**, 264–274 (2003)
59. S.-Y. Chen, B.W. Van Der Meer, *Biophys. J.* **64**, 1567–1575 (1993)
60. V. Martinez-Martinez, C. Corcostegui, J.B. Prieto, L. Gartzia, S. Salleres, I.L. Arbeloa, *J. Mater. Chem.* **21**, 269–276 (2011)
61. F.L. Labarthe et al., *Phys. Chem. Chem. Phys.* **2**, 5154–5167 (2000)
62. M. Richard-Lacroix, Ch. Pellerin, *Macromolecules* **45**, 1946–1953 (2012)
63. F.L. Labarthe, T. Buffeteau, C. Sourisseau, *J. Phys. Chem. B* **102**, 5754–5765 (1998)
64. E. Chrzumnicka, M. Szybowski, D. Bauman, *Z. Naturforsch.* **59a**, 510–516 (2004)
65. Sh Jen, N.A. Clark, P.S. Pershan, *J. Chem. Phys.* **66**, 4635–4661 (1977)
66. L.G.P. Dalmolen, S.J. Picken, A.F. de Jong, W.H. de Jeu, *J. Physique* **46**, 1443–1449 (1985)
67. A. Sanchez-Castillo, M.A. Osipov, F. Giesselmann, *Phys. Rev. E* **81**, 021707 (2010)
68. J. Purvis, D.I. Bower, *J. Polym. Sci. Polym. Phys. Ed.* **14**, 1461–1484 (1976)
69. N. Bielejewska et al., *Acta Phys. Pol. A* **110**, 777–793 (2006)
70. S.H. Patel et al., *Macromolecules* **48**, 6606–6616 (2015)

71. G.M. Su, S.H. Patel, C.D. Pemmaraju, D. Prendergast, M.L. Chabiny, *J. Phys. Chem. C* **121**, 9142–9152 (2017)
72. K. Weiss, Ch. Woll, D. Johannsmann, SPIE. Conference. Liq. Crystals III **3800**, 104–111 (1999)
73. T. Sakai, K. Ishikawa, H. Takezoe, N. Matsuie, Y. Yamamoto, H. Ishii, Y. Ouchi, H. Oji, K. Seki, *J. Phys. Chem. B* **105**, 9191–9195 (2001)
74. E. Morikawa, V. Saile, K.K. Okudaira, Y. Azuma, K. Meguro, Y. Harada, K. Seki, S. Hasegawa, N. Ueno, *J. Chem. Phys.* **112**, 10476–10481 (2000)
75. T. Hemraj-Benny et al., *Phys. Chem. Chem. Phys.* **8**, 5038–5044 (2006)
76. C. Lenardi et al., *J. Appl. Phys.* **85**, 5038–5044 (1999)
77. K. Weiss, Ch. Woll, D. Johannsmann, *J. Chem. Phys.* **113**, 11297–11305 (2000)
78. N. Kawatsuki, Y. Inada, M. Kondo, Y. Haruyana, Sh. Matsui, *Macromolecules* **47**, 2080–2087 (2014)
79. A. Prasad, R. Shroff, S. Rane, G. Beaucage, *Polymer* **42**, 3103–3113 (2001)
80. H.H. Chuah, B.T.A. Chang, *Polym. Bull.* **46**, 307–313 (2001)
81. M.T. Sims, L.S. Abbott, R.M. Richardson, J.M. Goodby, J.N. Moore, *Liq. Cryst.* **46**, 11–24 (2018)
82. ThT Mills, G.E.S. Toombes, S. Tristram-Nagle, G.W.F. Smilgies, J.F. Nagle, *Biophys. J.* **95**, 669–681 (2008)
83. A.J. Leadbetter, P.G. Wrighton, *J. Phys. Colloq.* **40**, 234–242 (1979)
84. N.S. Murthy, *Rigaku. J.* **21**, 15–24 (2004)
85. S. Murakami, Y. Nishikawa, M. Tsuji, A. Kawaguchi, S. Kohjiya, M. Cakmak, *Polymer* **36**, 291–297 (1995)
86. P. Landois et al., *Phys. Status Solidi B* **248**, 2449–2453 (2011)
87. T. Ito, Y. Maruhashi, M. Demura, T. Asakura, *Polymer* **41**, 859–866 (2000)
88. K. Schmidt-Rohr, H.W. Spiess, *Multidimensional Solid-State NMR and Polymers* (Academic Press, Harcourt Brace and Company, Publishers, London, San Diego, New York, Boston, Sydney, Tokyo, Toronto, 2005), 478 p
89. B.F. Chmelka, K. Schmidt-Rohr, H.W. Spiess, *Macromolecules* **26**, 2282–2296 (1993)
90. B.Q. Sun, J.H. Baltisberger, Y. We, A. Samoson, A. Pines, *Solid State Nucl. Magn. Reson.* **1**, 267–295 (1992)
91. P. Diehl, C.L. Khetrpal, H.P. Kellerhals, *Mol. Phys.* **15**, 333–337 (1968)
92. P. Diehl, P.M. Henrichs, W. Niederberger, *Mol. Phys.* **20**, 139–145 (1971)
93. Ph Lesot, Y. Gounelle, D. Meriet, A. Loewenstein, J. Courtieu, *J. Phys. Chem.* **99**, 14871–14875 (1995)
94. R. Hentschel, J. Schlitter, H. Sillescu, H.W. Spiess, *J. Chem. Phys.* **68**, 56–66 (1978)
95. H.W. Spiess, H. Sillescu, R. Hentschel, *Polymer* **22**, 1516–1521 (1981)
96. G.S. Harbison, V.-D. Vogh, H.W. Spiess, *J. Chem. Phys.* **86**, 1206–1218 (1987)
97. J.J. Titman, S.F. de Lacroix, H.W. Spiess, *J. Chem. Phys.* **98**, 3816–3826 (1993)
98. P.M. Henrichs, *Macromolecules* **20**, 2099–2112 (1987)
99. D.L. Tzoi, T.H. Huang, A.S. Abhiraman, R. Desai, *Polymer* **33**, 426–428 (1992)
100. R. Schreiber, W.S. Veeman, *Macromolecules* **32**, 4647–4657 (1999)
101. H. Menge, P. Ekanayake, M.E. Ries, M.G. Brereton, M. Findeisen, *Polym. Bull.* **43**, 371–378 (1999)
102. M.E. Ries et al., *Macromolecules* **32**, 4961–4968 (1999)
103. M. Wendlandt, J.B. van Beek, U.W. Suter, B.H. Meier, *Macromolecules* **38**, 8372–8380 (2005)
104. M. Wendlandt, Th.A. Tervoort, J.B. van Beek, U.W. Suter, *J. Mech. Phys. Solids* **54**, 589–610 (2006)
105. A.P.M. Kentgens, A.F. de Jong, E. de Boer, W.S. Veeman, *Macromolecules* **18**, 1045–1048 (1985)
106. S. Alexander, A. Baram, Z. Luz, *Mol. Phys.* **27**, 441–445 (1974)
107. M.M. Maricq, J.S. Waugh, *J. Phys. Chem.* **70**, 3300–3316 (1979)
108. Y. Yang, A. Hagermeyer, H.W. Spiess, *Macromolecules* **22**, 1004–1006 (1989)
109. A.P.M. Kentgens, E. de Boer, W.S. Veeman, *J. Chem. Phys.* **87**, 6859–6866 (1987)
110. V. Domenici, *Pure. Appl. Chem.* **79**, 21–37 (2007)
111. G.R. Luckhurst, A. Sugimura, B.A. Timimi, *Mol. Cryst. Liq. Cryst.* **347**, 53–63 (2000)
112. G.R. Luckhurst, T. Miyamoto, A. Sugimura, B.A. Timimi, *Mol. Cryst. Liq. Cryst.* **347**, 147–156 (2000)
113. G.R. Luckhurst, B.A. Timimi, T. Miyamoto, A. Sugimura, *Mol. Cryst. Liq. Cryst.* **402**, 103–116 (2003)
114. G.R. Luckhurst, T. Miyamoto, A. Sugimura, B.A. Timimi, *J. Chem. Phys.* **116**, 5099–5106 (2002)

115. G.R. Luckhurst, A. Sugimura, B.A. Timimi, H. Zimmermann, *Liq. Cryst.* **32**, 1389–1396 (2005)
116. K. Moriya, T. Suuki, Sh. Yano, S. Miyajima, *J. Phys. Chem. B* **105**, 7920–7927 (2001)
117. L.J. Berliner, J. Reuben, *Biological Magnetic Resonance, Volume 8, Spin Labeling, Theory and Applications* (Plenum Press, New York, London, 1989), 650 p
118. P. Diechl, C.F. Schwerdtfeger, *Mol. Phys.* **17**, 417–423 (1969)
119. P.G. James, G.R. Luckhurst, *Mol. Phys.* **19**, 489–500 (1970)
120. A.Kh. Vorob'ev, S. Ferster, V.S. Gurman, *Russ. J. Phys. Chem.* **74**, 1867–1872 (2000)
121. H.R. Falle, G.R. Luckhurst, *J. Magn. Reson.* **3**, 161–199 (1970)
122. B.G. McFarland, H.M. McConnell, *Proc. Natl. Acad. Sci. USA* **68**, 1274–1278 (1971)
123. C. Zannoni, G.F. Pedulli, L. Masotti, A. Spini, *J. Magn. Reson.* **43**, 141–153 (1981)
124. G.R. Luckhurst, M. Setaka, R.N. Yeates, C. Zannoni, *Mol. Phys.* **38**, 1507–1520 (1979)
125. G.R. Luckhurst, M. Setaka, C. Zannoni, *Mol. Phys.* **28**, 49–68 (1974)
126. G.R. Luckhurst, C. Zannoni, *Proc. R. Soc. Lond. A* **353**, 87–102 (1977)
127. A.G. Redfield, *Adv. Magn. Reson.* **1**, 1–32 (1966)
128. G.R. Luckhurst, C. Zannoni, *Nature* **267**, 412–414 (1977)
129. I.V. Ovchinnikov, I.G. Bikhantaev, N.E. Domracheva, *Pis'ma v Zh. Eksp. Teor. Fiz.* **23**, 584–587 (1976)
130. V.N. Konstantinov, I.V. Ovchinnikov, N.E. Domracheva, *Zh. Strukt. Khimii* **25**, 19–27 (1982)
131. E.G. Boguslavsky, S.A. Prokhorova, V.A. Nadolniny, in *Novel Methods to Study Interface Layers*, ed. by D. Mobius, R. Miller (Elsevier, Amsterdam, New York, 2001), pp. 109–120
132. E.G. Boguslavsky, S.A. Prokhorova, V.A. Nadolniny, *Appl. Magn. Res.* **23**, 123–132 (2002)
133. J.H. Freed, in *Spin Labelling: Theory and Applications*, ed. by L.J. Berliner (Academic Press, New York, 1976), pp.53–132
134. D.J. Schneider, J.H. Freed, in *Biological Magnetic Resonance V. 8*, ed. by L.J. Berliner, J. Reuben (Plenum Press, New York, 1989), pp. 1–76
135. D.E. Budil, S. Lee, S. Saxena, J.H. Freed, *J. Magn. Reson. Series A* **120**, 155–189 (1996)
136. Zh. Liang, Y. Lou, J.H. Freed, L. Columbus, W.L. Hubbell, *J. Phys. Chem. B* **108**, 17649–17659 (2004)
137. Z. Zhang et al., *J. Phys. Chem. B* **114**, 5503–5521 (2010)
138. A.Kh. Vorobiev, T.S. Yankova, N.A. Chumakova, *Chem. Phys.* **409**, 61–73 (2012)
139. T.P. Burghardt, N.L. Thompson, *Biophys. J.* **48**, 401–409 (1985)
140. K. Ajtai, L. Poto, T.P. Burghardt, *Biochemistry* **29**, 7733–7741 (1990)
141. K. Ajtai, A. Ringle, T.P. Burghardt, *Biochemistry* **31**, 207–217 (1992)
142. K. Ajtai, T.P. Burghardt, *Biochemistry* **31**, 4275–4282 (1992)
143. A.Kh. Vorobiev, N.A. Chumakova, *J. Magn. Reson.* **175**, 146–157 (2005)
144. A.Kh. Vorobiev, N.A. Chumakova, in *Nitroxides Theory, Experiment and Applications*, ed. by A.I. Kokorin (INTECH, Rijeka, 2012), pp. 57–112
145. T.S. Yankova, N.A. Chumakova, D.A. Pomogailo, A.Kh. Vorobiev, *Liq. Cryst.* **40**, 1135–1145 (2013)
146. N.A. Chumakova, T.S. Yankova, K.E. Fairfull-Smith, S.E. Bottle, A.Kh. Vorobiev, *J. Phys. Chem. B* **118**, 5589–5599 (2014)
147. A.V. Bogdanov, A.Kh. Vorobiev, *J. Phys. Chem. B* **117**, 12328–12338 (2013)
148. A.V. Bogdanov, G.I. Proniuk, A.Kh. Vorobiev, *Phys. Chem. Chem. Phys.* **20**, 18340–18347 (2018)
149. A.V. Bogdanov, A.Yu. Bobrovsky, A.Kh. Vorobiev, *J. Polym. Sci. B Polym. Phys.* **57**, 819–825 (2019)
150. N.A. Chumakova, T.S. Yankova, A.Kh. Vorobiev, *Appl. Magn. Reson.* **33**, 117–126 (2008)
151. T.S. Yankova, N.A. Chumakova, A.Kh. Vorobiev, *Russ. J. Phys. Chem.* **85**, 695–701 (2011)
152. N.A. Chumakova, A.T. Rebrikova, A.V. Talyzin, N.A. Paramonov, A. Vorobiev, M.V. Korobov, *J. Phys. Chem. C* **122**, 22750–22759 (2018)
153. A.Kh. Vorobiev, A.V. Bogdanov, T.S. Yankova, N.A. Chumakova, *J. Phys. Chem. B* **123**, 5875–5891 (2019)
154. A.V. Bogdanov, A.Kh. Vorobiev, *Phys. Chem. Chem. Phys.* **18**, 31144–31153 (2016)
155. A.V. Bogdanov, R. Tamura, A.Kh. Vorobiev, *Chem. Phys. Lett.* **749**, 137432 (2020)
156. V. Strauch, M. Schara, *Polymer* **36**, 3435–3438 (1995)
157. B.R. Arnold, A. Euler, P.V. Poliakov, A.W. Schill, *J. Phys. Chem. A* **105**, 10404–10412 (2001)
158. Y.R. Kim, M. Lee, J.R.G. Thorne, R.M. Hochstrasser, J.M. Zeigler, *Chem. Phys. Lett.* **145**, 75–80 (1988)

159. S. Constantine, J.A. Gardecki, Y. Zhou, L.D. Ziegler, X. Ji, B. Space, *J. Phys. Chem. A* **105**, 9861 (2001)
160. C.J. Milne et al., *J. Phys. Conference Series* **190**, 012052 (2009)

Publisher's Note Springer Nature remains neutral with regard to jurisdictional claims in published maps and institutional affiliations.